

Growth kinetics of a single $\text{InP}_{1-x}\text{As}_x$ nanowire

Jean-Christophe Harmand,* Frank Glas, and Gilles Patriarche

CNRS-Laboratoire de Photonique et de Nanostructures, Route de Nozay, 91460 Marcoussis, France

(Received 22 April 2010; revised manuscript received 8 June 2010; published 28 June 2010)

Semiconductor nanowires offer additional properties and more flexibility for many potential applications. However the precise control of their growth is very challenging and much more complex than for two-dimensional layers. Here, we present a method which provides detailed information on their formation. The method is implemented with In(P,As) nanowires grown by Au-catalyzed molecular beam epitaxy. Controlled and periodic modulations of the incident vapor phase are generated. Due to these modulations, the nanowires show small and short oscillations of composition along their growth axis. These oscillations furnish a time scale which is recorded in the nanowire solid phase. The instantaneous growth rate and the total length of the nanowire at any time of the growth are accessible. The experimental data are fitted with models. The adatom diffusion lengths on the different surfaces and the chemical potentials in the adsorbed and liquid phases are extracted. It appears that the vapor flux intercepted by the nanowire sidewalls is the dominant contribution to their elongation. We discuss which contribution allows one initiating their growth from the catalyst drop.

DOI: [10.1103/PhysRevB.81.235436](https://doi.org/10.1103/PhysRevB.81.235436)

PACS number(s): 81.07.Gf, 81.10.Aj, 81.05.Ea, 81.15.Kk

I. INTRODUCTION

Semiconductor nanowires (NWs) have shown promising characteristics in many fields.¹⁻⁵ Their synthesis is presently investigated by several growth techniques including laser ablation, vapor phase epitaxy and molecular beam epitaxy (MBE). For most applications, the breakthrough of NWs will depend on the possibility to control their length, diameter, composition, and doping with sufficient accuracy. A major challenge is to form NWs which include heterostructures of chosen dimensions. This kind of objective requires a precise knowledge of the growth kinetics which appear much more complex for NWs than for standard two-dimensional (2D) layers. NW growth involves several specific mechanisms of varying significance depending upon the growth technique in use. First, in catalyst-assisted growth, precursor decomposition depends on the local surface chemistry. Second, at least two different surface orientations coexist during NW growth: the substrate surface and the NW sidewalls. These distinct surfaces intercept and collect the vapor flows under different angles. Third, the adatoms diffuse on these surfaces with different characteristic lengths. Fourth, the energy barrier for solid phase nucleation varies at the different surfaces and interfaces of the catalyst/NW/substrate system. The combination of these effects can lead to growth rates which are not constant with time, even at constant incoming precursor flows. In particular, the NW elongation with time (the axial growth rate) was observed to be sublinear⁶ or superlinear.⁶⁻⁸ Although these various phenomena have already been examined, they are not all satisfactorily described, understood and quantified. The present work provides an experimental contribution which allows one to determine finely the chronology of growth of individual NWs and to derive values of important growth-related parameters.

Most experimental studies evaluate the kinetics of NW growth from postgrowth measurements of final NW lengths at several given growth times.⁶⁻⁸ This is far from satisfactory since such measurements can hardly record the transient and nonlinear behaviors that have been predicted by several

models.⁷⁻⁹ More precise information can be derived from the use of markers consisting of thin layers of a chemically different material inserted in the NW.^{10,11} However, fine variations of growth rate are difficult to measure in this way and the insertion of the marker itself can alter the growth kinetics. Conversely, *in situ* transmission electron microscopy experiments¹² accurately record instantaneous growth rates and changes of NW or droplet morphologies but they are currently limited in terms of growth methods and material systems (group IV semiconductors). In this work, we propose and demonstrate a simple method to investigate finely the growth of a single NW. Our study, which focuses on molecular beam epitaxy (MBE) of III-V compounds, shows that NW elongation is highly nonlinear with time. This behavior reflects the crucial role of the sidewall facets that intercept the incoming vapor fluxes. Existing models are adapted to fit our experimental data and to evaluate important parameters.

II. EXPERIMENTAL

Our method relies on small periodic modulations of the incident vapor fluxes, produced on purpose. The amplitude and the time period of the flux modulation are fixed experimentally and chosen to produce small but detectable changes in the NW composition along the growth direction. The growth kinetics is determined by counting the number of monolayers formed during each time period of the modulation. We used this method recently to study the nucleation statistics at the liquid catalyst/solid NW interface.¹³ Obviously, for III-V compounds, a ternary alloy at least is necessary to obtain the composition modulation. Here, the method is implemented on $\text{InP}_{1-x}\text{As}_x$ NWs grown at 420 °C by Au-catalyzed MBE on (111)*B* oriented InP substrates. Our growth conditions produce NWs of wurtzite structure which grow in the [0001] direction without stacking faults. As_4 and P_2 fluxes are evaporated from solid sources and a periodic modulation of the incident $\text{As}_4:\text{P}_2$ flux ratio is produced. The flux modulations may be obtained either by directly modu-

lating the sources or indirectly. In the present study, we use the second method: the modulation is obtained at constant source fluxes, by exploiting the geometry of the MBE growth chamber, namely, the fact that the molecular beams are not perfectly uniform on the wafer area. When the substrate is rotating, the NWs situated close to its periphery experience a small modulation of the incoming fluxes during one substrate rotation. The flux modulation amplitude varies along the wafer radius, from 0 at the wafer center to about 15% of the average flux at the edge of a 2 in wafer. The NWs presented here were sampled at 5 mm from the edge.

Several important conditions must be met in order to transfer the flux modulation to an axial modulation of the NW composition. First, several monolayers must grow within one modulation time period. We chose a time period of 3.6 s corresponding to the growth of about 10 to 30 monolayers. The corresponding length (3–10 nm) is sufficiently small to probe finely the growth kinetics. Second, we must avoid a complete damping of the flux modulation upon transferring atoms into the liquid drop, which acts as a reservoir. In this respect, the high solubility of group III atoms in the catalyst is not favorable. Modulating the group V flux is expected to be more appropriate since P and As are much less soluble in the catalyst. On the other hand, the modulation must be small enough to minimize the resulting perturbation on NW growth kinetics.

The NWs analyzed in the following have uniform diameter, close to the size of the catalyst particle. This morphology indicates that nucleation at the NW sidewalls is negligible. Hence, the present experiments probe the sole axial growth. The $\text{InP}_{1-x}\text{As}_x$ NWs grown with modulated beams were removed from their substrate, deposited on a thin silicon nitride membrane and imaged by high angle annular dark field (HAADF) scanning transmission electron microscopy (STEM). This technique is very sensitive to composition variations.¹⁴ The images were obtained in a 200 kV field emission gun JEOL 2200FS microscope, equipped with a spherical aberration corrector for the probe. The probe had the following characteristics: 50 pA current, 0.1 nm size, and 30 mrad semiangle. The inner and outer collection angles of the HAADF detector were 100 and 170 mrad, respectively. The image of a NW segment of 45 nm diameter is presented in Fig. 1.

The faint contrast along the growth axis reveals that the composition of this NW has indeed been modulated. The modulation of the HAADF intensity profile integrated over the whole diameter is superimposed [Fig. 1(a)]. A fast-Fourier-transform (FFT) filtered HAADF image with the corresponding intensity profile is also shown [Fig. 1(b)]. The oscillation amplitude is about $\pm 0.7\%$ of the total HAADF intensity. The corresponding variation Δx of the As concentration x was determined by energy dispersive x-ray spectroscopy (EDXS) to be about ± 0.03 around the mean value of 0.66. An estimate based on Rutherford scattering indicates that the observed HAADF intensity oscillation amplitude is consistent with this composition excursion.

The distance between two concentration extrema equals the increase of NW length during one time period. Therefore, it is straightforward to determine the instantaneous growth rate at each oscillation. The complete chronology of the NW

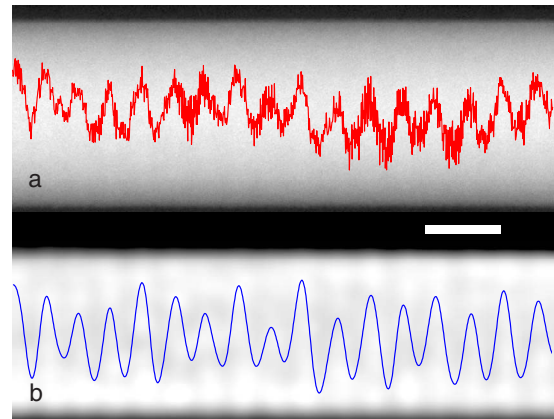


FIG. 1. (Color online) Modulation of composition in an $\text{InP}_{1-x}\text{As}_x$ nanowire segment grown with a modulated $\text{As}_4:\text{P}_2$ flux ratio. HAADF STEM image of the nanowire segment observed along the $\langle \bar{2}110 \rangle$ zone axis. The scale bar represents 20 nm. (a) The HAADF signal is integrated over the whole diameter and the profile is plotted along the growth axis. (b) Fast-Fourier-transform filtered HAADF image and corresponding profile.

growth is thus accessible. In the present experiments, since the foot of the NW gets buried by the layer growing between the NWs and since the NWs get cleaved before TEM examination, the bottom part of the NW is not observed. However, counting the oscillations from a reference point deliberately introduced in the growth sequence allows one dating the exact time at which each oscillation was formed. This procedure was applied to a 21 nm diameter NW. The entire NW, from the cleaved end to the catalyst particle, was monitored by using six HAADF overlapping images precisely positioned with respect to each other by superimposing any remarkable detail common to two of them. The HAADF intensity profiles were treated with a FFT bandpass filter in order to reduce noise and to extract the positions of the oscillation maxima. We finally obtained the dependence with time of the NW height counted from the cleaved end, as presented in Fig. 2.

The measured height of the NW displays a nonlinear behavior which will be discussed in Secs. III and IV. Before that, we comment two particular features. First, in this growth experiment, we stopped the flux modulation for 12 time periods. Consequently a short segment of the NW does not present regular composition oscillations. As mentioned above, the corresponding region, indicated in Fig. 2, may serve as a time reference. Second, at some point during growth, the nominal $\text{As}_4:\text{P}_2$ ratio was changed abruptly from 1:5 to 3:3 while the total average group V flux was kept constant. Thanks to the former time reference, this event can be accurately dated, as shown in Fig. 2. The impact of this large change of flux ratio is strong and immediate: as seen from the change of slope in Fig. 2, the growth rate was suddenly reduced by a factor 2. This behavior contrasts much with the case of conventional MBE growth of two-dimensional (2D) layers, for which the growth rate is fixed by the sole group III elements.

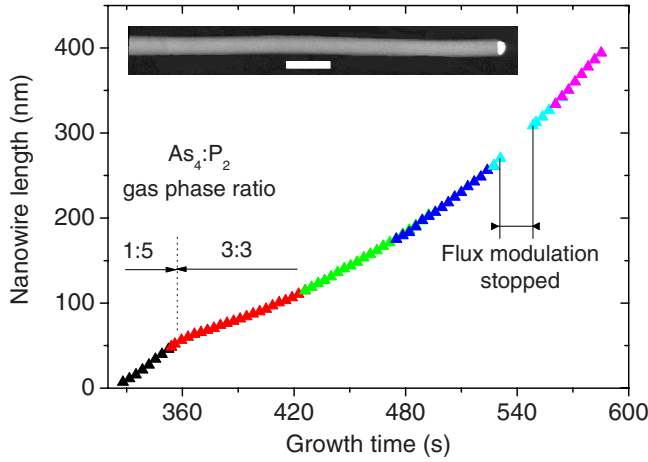


FIG. 2. (Color online) Chronology of growth of a single $\text{InP}_{1-x}\text{As}_x$ nanowire. The length of the nanowire shown in the inset (scale bar: 50 nm), is measured from its cleaved edge and plotted as a function of the absolute growth time, as deduced from the composition oscillations along its axis. The different colors correspond to different overlapping HAADF images. During the growth experiment, the flux modulation was stopped for 12 time periods. The corresponding region, where composition oscillations are missing, serves as a time reference. At 355 s, the nominal $\text{As}_4:\text{P}_2$ flux ratio was changed abruptly from 1:5 to 3:3.

III. MODELS

We now analyze the experimental dependence of the NW height. Several models⁷⁻⁹ have predicted nonlinear effects in NW axial growth. These models consider three material flows contributing to NW growth: (i) direct impingement on the drop, (ii) direct impingement on the sidewalls followed by diffusion to the drop, (iii) impingement on the substrate surface and diffusion to the drop along the sidewalls. The growth rate is then determined by solving a balance equation. For III-V alloys, this procedure can be applied to each component. In MBE, the problem is simpler for the group III species which are elemental in the vapor or physisorbed states. Moreover, in a large range of growth temperature, their desorption rate from the substrate is negligible as compared to the incoming flux. In their present development, the models considered are limited by the implicit assumption that the liquid drop state is stationary. Since the NW growth rate is not constant, this stationary condition cannot be strictly verified: droplet composition and supersaturation evolve as growth is pursued. Nevertheless, it is instructive to apply these models to evaluate, in a first approximation, the respective importance of contributions (i), (ii), and (iii).

A. Phenomenological model

We first analyze our experimental data with a model adapted to our experimental conditions from those developed by Tchernycheva *et al.*⁷ and Plante and LaPierre.⁸ The balance equation is solved for the In atoms and their re-evaporation from the $\text{InP}(\text{As})$ surfaces at 420 °C is neglected. We consider J , the beam flux of In atoms impinging on the sample ($J=3.96 \text{ nm}^{-2} \text{ s}^{-1}$) at an angle α with respect

to the substrate normal ($\alpha=32.5^\circ$). We call R the NW radius ($R=10.5 \text{ nm}$ for the NW of Fig. 2) and L^2 the mean substrate area per NW (the reverse of the NW surface density). The catalyst droplet has a contact angle β with respect to its horizontal base plane. The sample under study has a low NW density ($L=300 \text{ nm}$), hence shadowing between NWs is negligible.

The total number of group III atoms impinging on the sample area L^2 per unit time is $T=L^2J \cos \alpha$. The part of these atoms which is intercepted by the catalyst droplet on top of the NW writes $A=a\pi R^2J$ where a is a dimensionless geometrical factor depending on angles α and β . Approximate expressions for this parameter were used in previous works.^{7-9,15} Here we take the exact expression of a determined by Glas¹⁶ (in the present case, its value is very close to $\sin^{-2} \beta$). We consider that this part A is fully incorporated into the NW and we shall see that it plays an important role in NW growth initiation. Since A depends on β , it is important to evaluate the contact angle during growth. For the NW under study, postgrowth measurements at room temperature indicate that β is about 100° and that the drop composition, determined by EDXS, is $\text{In}_{0.33}\text{Au}_{0.67}$. During growth, the drop must contain more In along with small amounts of As and P to insure the supersaturation of these constituents. On the other hand, we assume that the amount of Au in each droplet is unchanged when cooling the sample. According to our thermodynamical calculations,¹⁷ assuming that As and P represent about 2% of the drop composition during growth,¹³ an In concentration of about 60% leads to a supersaturation in the liquid phase of about 300 meV per III-V pair,¹⁷ a reasonable value consistent with the observed NW growth rate.¹³ Taking into account the drop inflation necessary to accumulate these extra atoms, the contact angle β during growth would then be close to 120° . This latter β value is used hereinafter.

A second part of the incoming atoms (ii) is intercepted by the NW sidewalls and we assume that a fraction b of these can diffuse to the catalyst droplet and effectively contributes to NW elongation. This contribution writes $B=2bRH_W(t)J \sin \alpha$, where $H_W(t)$ is the apparent NW height emerging at time t from the 2D layer which grows between the NWs. The third contribution to NW elongation stems from the collection of adatoms from the substrate surface followed by their migration to the drop. As in Ref. 8, we assume that these atoms are collected from a ring of width l and area \mathcal{A} surrounding the NW, hence $C=\mathcal{A}J \cos \alpha$, with $\mathcal{A}=\pi l(l+2R)$. The NW elongation results from the sum of the three contributions:

$$\begin{aligned} \frac{dH_T(t)}{dt} &= \frac{\Omega}{\pi R^2}(A+B+C) \\ &= J\Omega \left\{ a + b \frac{2}{\pi R} H_W(t) \sin \alpha + \frac{\mathcal{A}}{\pi R^2} \cos \alpha \right\} \quad (1) \end{aligned}$$

where $H_T(t)$ is the total NW length measured from a fixed reference, namely, the initial substrate-NW interface, and Ω is the volume per group III atom in the solid III-V compound. We consider that the atoms which do not participate in the NW elongation are incorporated at the substrate sur-

face and form the 2D layer which hence grows at the rate

$$\frac{dH_{2D}(t)}{dt} = \frac{\Omega}{L^2 - \pi R^2}(T - A - B - C) \approx J\Omega \cos \alpha - \frac{\pi R^2}{L^2} \frac{dH_T(t)}{dt}, \quad (2)$$

where, in the second equality, we have kept only the terms of lowest order in (R/L) . Equation (2) describes the fact that NWs grow to the detriment of 2D growth. For simplicity, previous works⁷⁻⁹ have considered a constant 2D growth rate equal to $J\Omega \cos \alpha$. The correction included in Eq. (2) easily amounts to several percent of this nominal growth rate, even at the modest NW density and small NW radius considered here. In most realistic cases, this correction cannot be neglected. The 2D layer buries progressively the bottom of the NW. Therefore, the height of the emerging part of the NW is $H_W(t) = H_T(t) - H_{2D}(t)$ and, using Eq. (2), its variation with time writes:

$$\frac{dH_W(t)}{dt} = \frac{dH_T(t)}{dt} \left(1 + \frac{\pi R^2}{L^2} \right) - J\Omega \cos \alpha \quad (3)$$

Combining Eqs. (1) and (3) gives a differential equation which is solved to fit our experimental data (Fig. 2). For both growth conditions (low and high $As_4:P_2$ ratio), we have two adjustable parameters, namely b and \mathcal{A} (or l , since R is fixed). The first part of growth (low $As_4:P_2$ ratio) can be very well fitted with $b=1$ and $l=0.5$ nm. This means that all the In atoms collected by the sidewalls are transferred to the drop and participate in NW axial growth, while the collection of substrate surface adatoms contributes very marginally to NW elongation (l is very small). In the second part of growth (high $As_4:P_2$ ratio), b must be taken less than 1. Since In desorption is negligible, this indicates that part of the adatoms collected by the NW sidewalls now diffuse to the substrate. This part corresponds to the adatoms intercepted by a NW portion of length $(1-b)H_W$ and, for sake of consistency, we must have $C=0$. In these conditions, the model cannot fit the data satisfactorily (see Fig. 3(a) and Table I). However, the fit is much improved if we allow contribution C to be negative. The former expression of C is then replaced by $-\mathcal{A}'J \sin \alpha$ where $\mathcal{A}'=2Rh$ is now the cross-sectional area of the lowest portion of NW of height h from which adatoms flow to the substrate. Accordingly, H_W is replaced by $H_W - h$ in the expression of B . This means that the flow of adatoms from the sidewalls to the substrate now corresponds to the effective collection height $h + (1-b)(H_W - h) = bh + (1-b)H_W$ while the flow to the catalyst corresponds to $b(H_W - h)$. An excellent agreement is obtained for the second part

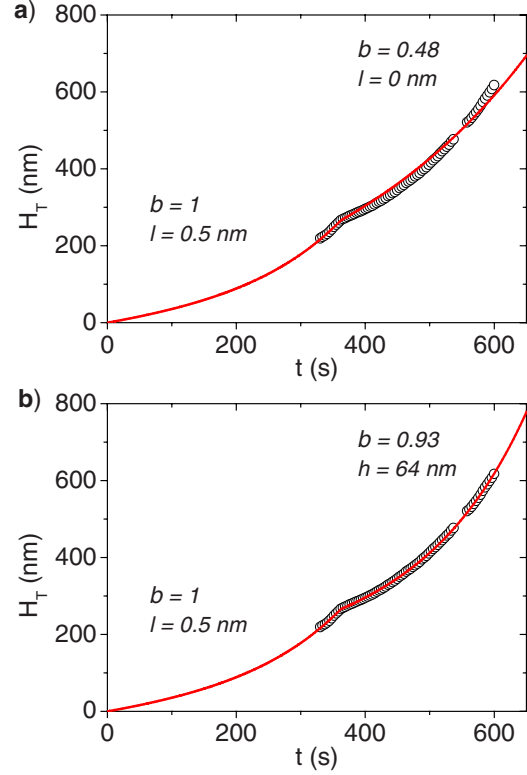


FIG. 3. (Color online) Experimental NW elongation (circles) fitted with a model adapted from Refs. 7 and 8 (lines), with different parameters for each $As_4:P_2$ ratio, before and after $t=355$ s. Two sets of parameters are compared for the second growth stage: (a) no collection of substrate adatoms ($l=0$ nm); (b) adatom flow from NW to substrate surface ($h=64$ nm).

of growth with $b=0.93$ and $h=64$ nm [Fig. 3(b)]. Thus, in this second growth stage, the adatoms collected by the sidewalls are shared between NW and 2D layer growth. At $H_W = 500$ nm, the effective collection height for diffusion to the substrate amounts to 94.5 nm.

B. Diffusion model

These preliminary conclusions are useful for implementing the model of Dubrovskii *et al.*⁹ which describes more accurately the migration of adatoms on the different surfaces, at the expense of more unknown parameters. In this model, the diffusion equations are solved with adequate boundary conditions. In order to minimize the number of parameters, we reformulate the expression of NW elongation with time found in Ref. 9 as follows:

$$\frac{dH_T(t)}{dt} = J\Omega \left[a + \frac{\left\{ \frac{2\lambda_f}{\pi R}(1 - \varepsilon_f)\sin \alpha \right\} U\left(\frac{H_W(t)}{\lambda_f}\right) + \left\{ \frac{2\lambda_s}{R}(1 - \varepsilon_s)\delta \cos \alpha \right\}}{U'\left(\frac{H_W(t)}{\lambda_f}\right)} \right]. \quad (4)$$

TABLE I. Parameters and standard deviations corresponding to the fit of Fig. 3 with a model adapted from Refs. 7 and 8. b is the fraction of adatoms intercepted by the NW sidewalls which diffuses to the catalyst droplet, C is a constant flow of adatoms from the substrate surface to the NW with the following characteristic lengths of collection: l on the substrate if $C \geq 0$, or h on the NW if $C < 0$. Standard deviations between calculation and experiment are indicated for the first part of growth (σ_1) and for the full dataset (σ_T).

	b	Sign of C	l or h (nm)	σ_1 (nm)	σ_T (nm)
First part of growth	1	+	0.5	1.19	
Second part of growth	0.48	0	0		12.34
First part of growth	1	+	0.5	1.19	
Second part of growth	0.93	-	64		1.28

In this expression, λ_s and λ_f are the adatom diffusion lengths on the substrate surface and on the sidewalls, respectively. k being the Boltzmann's constant and T the growth temperature, we have $\varepsilon_s = \exp(-\Delta\mu_{sl}/kT)$ and $\varepsilon_f = \exp(-\Delta\mu_{fl}/kT)$ with $\Delta\mu_{sl} = \mu_s - \mu_l$ and $\Delta\mu_{fl} = \mu_f - \mu_l$, where μ_l and μ_s are the chemical potentials per III-V pair in the liquid droplet and at the substrate surface far from the NW; μ_f is the chemical potential on the sidewall at the maximum possible adatom coverage of the latter (limited by desorption only). The parameter δ equals $K_1(R/\lambda_s)/K_0(R/\lambda_s)$ where K_i is the modified Bessel function of the second kind of order i . The function $U(x)$ is given by $U(x) = \sinh x + \nu\delta(\cosh x - 1)$ and $U'(x) = \cosh x + \nu\delta \sinh x$, with $\nu = \lambda_s \varepsilon_s \pi / (\lambda_f \varepsilon_f \tan \alpha)$. Eq. (1) of the former model is replaced by Eq. (4) where modified expressions of contributions B (second term) and C (third term) appear. Eq. (2) and (3) remain valid to express the 2D layer and apparent NW growth rates.

We now have four adjustable parameters for each growth stage: $\Delta\mu_{sl}$, $\Delta\mu_{fl}$, λ_s , and λ_f . To reduce the number of free parameters, we keep the same value of λ_f for both growth stages. Although we recently showed that the group V species can affect this diffusion length,¹⁸ in the present case λ_f has little influence on the calculation, provided that it is larger than the final NW length, as shown later. We take $\lambda_f = 2 \mu\text{m}$, a reasonable value since in our conditions, NWs up to this length can be obtained without radial growth. Concerning λ_s , we find that very small values (a few nm) are necessary to fit the experiment, consistently with the low l value obtained in the previous model. Our best fit is obtained with $\lambda_s = 2 \text{ nm}$. This very short length is surprising at first sight, but it can be understood as a limitation of adatom diffusion by atomic steps. Indeed, the epilayer between the NWs has an ample surface roughness and the widths of the terraces between the atomic steps can be as small as a few nm. In these conditions, changing the group V flux is also expected to have little impact on the substrate surface diffusion. For that reason, we use the same value of λ_s for both growth stages. On the other hand, the abrupt change of $\text{As}_4:\text{P}_2$ flux ratio is expected to modify significantly the composition and the chemical potential of the catalyst droplet. Accordingly, we adjust two sets of chemical potential differences, valid before and after this change. We find $\Delta\mu_{fl} = 270 \text{ meV}$ and $\Delta\mu_{sl} = 18.2 \text{ meV}$ for the first part of growth, indicating net flows of adatoms diffusing from the sidewall facets and from the substrate surface to the droplet.

As in the former model, the contribution from the substrate surface is very small due to the combination of low λ_s and moderate $\Delta\mu_{sl}$. Very quickly, the contribution from the sidewalls dominates largely. After the change of $\text{As}_4:\text{P}_2$ flux ratio, $\Delta\mu_{fl}$ must be reduced to 160 meV, which indicates that the flow from the sidewalls to the droplet is less efficient when P_2 is replaced by As_4 . At the same time, $\Delta\mu_{sl}$ takes a negative value of -145 meV, showing that a significant part of the atoms intercepted by the NW now migrates to the substrate surface, to the detriment of NW growth. This behavior is in line with the conclusions derived from the former model. This illustrates the crucial role of group V fluxes which can, via their interaction with the other constituents of the drop, affect the chemical potential of In in the latter¹⁷ and redirect part of the diffusion flow of In adatoms. With these parameters, Dubrovskii's model describes fairly well the experimental dependence $H_T(t)$, and the abrupt change in NW growth rate is well reproduced, as shown in Fig. 4.

IV. DISCUSSION

We derive important conclusions from these results. In our experiments, NW growth is mainly sustained by contributions A and B . As the NW aspect ratio becomes significant, contribution A tends to be marginal as compared to B . The latter is responsible for the nonlinear variation of $H_T(t)$: as the NW becomes longer, it collects more material on its sidewalls and consequently grows faster. During the first growth stage, almost all the In atoms intercepted by the NW sidewall facets are transferred to the catalyst droplet. During the second stage, this transfer is less efficient as a consequence of the change of $\text{As}_4:\text{P}_2$ ratio which affects the drop chemistry. The concentrations of As and P in the drop are modified and their interactions with the other constituents of the liquid phase have a significant impact on the chemical potentials in the liquid.¹⁷ Since the As and P concentrations in the drop are low, its composition may change rapidly. Only a few monolayers are grown during the corresponding transient regime which therefore appears as a growth rate discontinuity [see Fig. 4(b)].

Contribution C is close to zero or even negative. This conclusion goes against the prevailing idea that collection of substrate adatoms is necessary to explain NW growth. Let us show that NW growth can even be initiated without this lat-

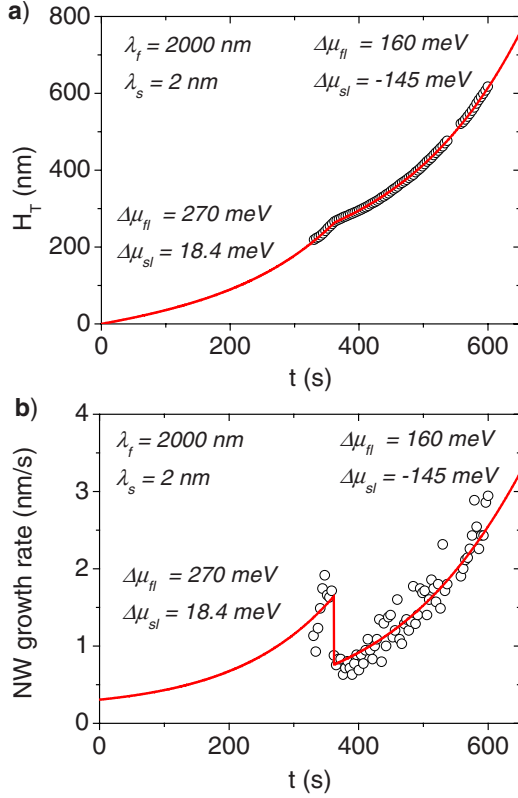


FIG. 4. (Color online) Experimental NW elongation and corresponding axial growth rate (circles) fitted with a model adapted from Ref. 9 (lines) and a reduced number of free parameters (λ_f , λ_s , $\Delta\mu_{fI}$, and $\Delta\mu_{sI}$). Different chemical potential differences are used for each $\text{As}_4:\text{P}_2$ ratio, before and after $t=355$ s.

ter contribution (without excluding that this contribution can play some role). We consider the catalyst drop as a truncated sphere sitting on the substrate with the contact angle β . The sidewalls are not yet formed ($B=0$), and we assume that $C=0$. The drop intercepts the vapor flux aJ while the substrate surface receives flux $J \cos \alpha$. Thus, if $a/\cos \alpha > 1$, more In is supplied to the liquid/solid interface via the drop as compared to the flux impinging on the rest of the substrate surface. This condition is satisfied as soon as $\beta > \frac{\pi}{2} - \alpha$, which is very likely the case in our experiments. This geometrical effect, first highlighted by Chatillon *et al.*,¹⁵ is thus sufficient to explain how NW growth starts. Note that if β is temperature-dependent and becomes less than $\frac{\pi}{2} - \alpha$ above a certain temperature, NW formation could be hindered while 2D growth would still be possible. This could explain why experiments show that InAs or InP NW growth cannot be initiated at $T > 450$ °C.⁷

The NW sidewall facets consist of $\{\bar{2}110\}$ planes. At a given time, the chemical potential on these facets has a certain profile along z , with a maximum value, μ_{max} , situated at altitude \hat{z} (μ_{max} tends toward μ_f for an infinitely long NW). Let us call j_b and j_t the diffusion fluxes of adatoms at the bottom and at the top of the NW (counted positive if directed upwards). In the first growth stage, j_b and j_t are positive and μ_{max} is located at the bottom of the NW ($\hat{z}=0$). In the second stage, j_b is negative and in that case the diffusion equation on

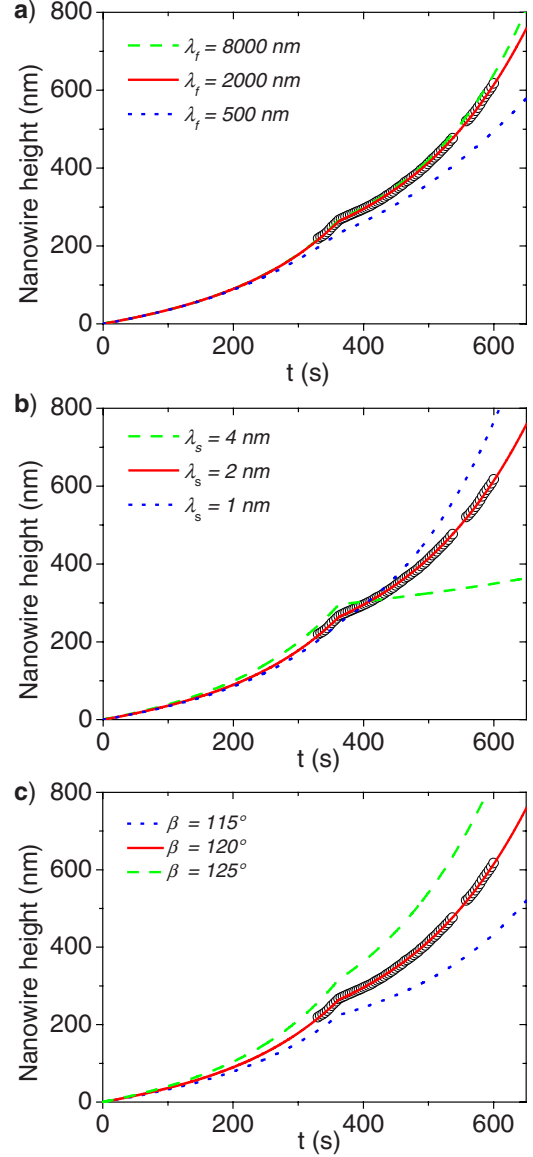


FIG. 5. (Color online) Influence of several parameters on the calculated NW elongation with time. (a) Influence of diffusion length on the NW sidewalls, λ_f ; (b) influence of the diffusion length on the substrate surface, λ_s ; (c) influence of the contact angle of the catalyst droplet, β .

the sidewalls leads to $\hat{z} = \frac{\lambda_f}{2} \ln \left[\frac{j_b \exp(H_W/\lambda_f) - j_t}{j_b \exp(-H_W/\lambda_f) - j_t} \right]$. As long as H_W is less than λ_f , \hat{z} varies slowly with H_W and, if $H_W \ll \lambda_f$, we have $\hat{z} \approx H_W j_b / (j_b - j_t)$. For $H_W=500$ nm, we obtain $\hat{z} = 113.7$ nm. This value is comparable to the effective collection height of 94.5 nm which was extracted using the first model from the estimate of the portion of adatoms diffusing from the sidewalls to the substrate. \hat{z} corresponds to the sidewall altitude where the In adatom concentration is highest and this local concentration increases as the NW grows. At NW heights longer than those investigated here, the nucleation on these $\{\bar{2}110\}$ facets likely occurs near \hat{z} and radial growth can develop by step flow parallel to the facets.⁸

Our study is limited to stationary values of μ_t , the chemical potential in the liquid. Further developments should in-

TABLE II. Parameters and standard deviations corresponding to the experimental data of Fig. 3 with a model adapted from Ref. 9. Standard deviations between calculation and experiment are indicated for the first part of growth (σ_1) and for the whole data (σ_T).

	λ_f (nm)	λ_s (nm)	$\Delta\mu_{fl}$ (meV)	$\Delta\mu_{sl}$ (meV)	σ_1 (nm)	σ_T (nm)
First part of growth	2000	2	270	160	1.40	
Second part of growth	2000	2	18.4	-145		2.00
First part of growth	2000	25	150	1.42	1.60	
Second part of growth	2000	25	135	-21.8		3.40
First part of growth	2000	200	90	0.2	5.18	
Second part of growth	2000	200	260	-0.21		9.99

clude its increase with time which must account for the increase of NW growth rate.

V. PARAMETERS ROBUSTNESS

We examine the robustness of the set of parameters used to fit the experimental data. As mentioned before, changing λ_f has little influence on the calculation provided that its value is higher than the NW height. This is illustrated in Fig. 5(a). The calculation is more sensitive to λ_s [Fig. 5(b)]. Our best fit is obtained with a very short λ_s , about an order of magnitude smaller than the diffusion length used by Dubrovskii *et al.* to fit their experimental dependence of GaAs NW length with R .¹⁹ The latter NWs were grown at 560 °C, i.e., 140 °C higher than the present In(As,P) NWs. This could partly explain the difference. Nevertheless, the robustness of our parameters has been tested by optimizing the chemical potential differences with different values of λ_s . Table II summarizes the fitting parameters and gives the standard deviations between calculated and experimental data. A reasonable fit can be obtained with $\lambda_s=25$ nm and significant changes on the chemical potential differences. However, this new set of parameters does not alter the direction of adatom flows. On the contrary, if λ_s is set to a few hundred of nm, it is impossible to obtain a good fit.

The influence of β is illustrated in Fig. 5(c). The calculation is very sensitive to this parameter. As explained in Sec. IV, β influences the initial axial growth rate which is mainly fixed by contribution A. A change of 5° around $\beta=120^\circ$ produces a 10% variation of the initial growth rate. Since the NW elongation is exponential-like, this modest difference is amplified with time. Apart from the few *in situ* TEM observations, β cannot be measured during NW growth. Our work points out that this parameter has to be carefully estimated to minimize the uncertainty which affects the other parameters of the models.

VI. CONCLUSION

Much information on nanowire growth can be derived from the experimental method presented here. The modulations of composition are similar to the rings of a tree which inform on the chronology of its growth. Incidentally, the radial growth of a nanowire could also be investigated with the same principle. Since the method relies on chemical composition, it can be applied to any crystalline orientation. It is all the more sensitive when the concentration of a heavy element is modulated in a light matrix alloy. Existing models can reproduce fairly well the time dependence of NW elongation in the particular case of our Au catalyzed MBE grown In(As,P) NWs. Although they are presently limited to stationary chemical potentials of a single element (In in our case), these models allow one to derive important trends. At variance with what is often assumed, we find that the diffusion of In adatoms from the substrate surface to the NW is a minor contribution to NW growth. The net flow of adatoms can even follow the reverse direction, from the NW sidewalls to the substrate surface. The beam flux intercepted by the NW sidewalls represents the main contribution to NW growth. The contact angle of the catalyst drop is a critical parameter which, via its impact on the initial NW growth rate, affects the whole growth chronology. These conclusions evidence the high sensitivity of NW kinetics on geometrical factors.

ACKNOWLEDGMENTS

This work was partly realized within Agence Nationale de la Recherche Project No. BONAFO ANR-08-NANO-031. The authors would like to thank V. G. Dubrovskii for his critical reading of the paper and his helpful comments.

*jean-christophe.harmand@lpn.cnrs.fr

¹C. Thelander, P. Agarwal, S. Brongersma, J. Eymery, L. F. Feiner, A. Forchel, M. Scheffler, W. Riess, B. J. Ohlsson, U. Gösele, and L. Samuelson, *Mater. Today* **9**, 28 (2006).

²M. S. Gudiksen, L. J. Lauhon, J. Wang, D. C. Smith, and C. M. Lieber, *Nature (London)* **415**, 617 (2002).

³Y. Huang, X. F. Duan, and C. M. Lieber, *Small* **1**, 142 (2005).

⁴M. D. Kelzenberg, D. B. Turner-Evans, B. M. Kayes, and M. A.

- Filler, *Nano Lett.* **8**, 710 (2008).
- ⁵Y. Cui, Q. Wei, H. Park, and C. M. Lieber, *Science* **293**, 1289 (2001).
- ⁶S. A. Dayeh, E. T. Yu, and D. D. Wang, *Nano Lett.* **9**, 1967 (2009).
- ⁷M. Tchernycheva, L. Travers, G. Patriarche, F. Glas, J.-C. Harmand, G. E. Cirlin, and V. G. Dubrovskii, *J. Appl. Phys.* **102**, 094313 (2007).
- ⁸M. C. Plante and R. R. LaPierre, *J. Appl. Phys.* **105**, 114304 (2009).
- ⁹V. G. Dubrovskii, N. V. Sibirev, G. E. Cirlin, A. D. Bouravleuv, Y. B. Samsonenko, D. L. Dheeraj, H. L. Zhou, C. Sartel, J. C. Harmand, G. Patriarche, and F. Glas, *Phys. Rev. B* **80**, 205305 (2009).
- ¹⁰E. I. Givargizov, *J. Cryst. Growth* **31**, 20 (1975).
- ¹¹D. L. Dheeraj, G. Patriarche, H. Zhou, J. C. Harmand, H. Weiman, and B. O. Fimland, *J. Cryst. Growth* **311**, 1847 (2009).
- ¹²F. M. Ross, J. Tersoff, and M. C. Reuter, *Phys. Rev. Lett.* **95**, 146104 (2005).
- ¹³F. Glas, J. C. Harmand, and G. Patriarche, *Phys. Rev. Lett.* **104**, 135501 (2010).
- ¹⁴E. Carlino and V. Grillo, *Phys. Rev. B* **71**, 235303 (2005).
- ¹⁵C. Chatillon, F. Hodaj, and A. Pisch, *J. Cryst. Growth* **311**, 3598 (2009).
- ¹⁶F. Glas, *Phys. Status Solidi B* **247**, 254 (2010).
- ¹⁷F. Glas, *J. Appl. Phys.* (to be published).
- ¹⁸C. Sartel, D. L. Dheeraj, F. Jabeen, and J. C. Harmand, *J. Cryst. Growth* **312**, 2073 (2010).
- ¹⁹V. G. Dubrovskii, N. V. Sibirev, R. A. Suris, G. E. Cirlin, V. M. Ustinov, M. Tchernysheva, and J. C. Harmand, *Semiconductors* **40**, 1075 (2006).